Nanocharacterisation of precipitates in austenite high manganese steels with advanced techniques: HRSTEM and DualEELS mapping

J. Bobynko[1], A.J. Craven[1], D. McGrouther[1], I. MacLaren[1], and G. Paul[2]
1 Kelvin Nanocharacterisation Centre, SUPA School of Physics and Astronomy, University of Glasgow, Glasgow G12 8QQ, UK.

2 ThyssenKrupp Steel Europe AG, Research and Development, FuE-E Modelling and Simulation, Kaiser-Wilhelm-Straße 100, 47166 Duisburg, Germany

E-mail: Ian.MacLaren@glasgow.ac.uk

Abstract. To achieve optimal mechanical properties in high manganese steels, the precipitation of nanoprecipitates of vanadium and niobium carbides is under investigation. It is shown that under controlled heat treatments between 850°C and 950°C following hot deformation, few-nanometre precipitates of either carbide can be produced in test steels with suitable contents of vanadium or niobium. The structure and chemistry of these precipitates are examined in detail with a spatial resolution down to better than 1 nm using a newly commissioned scanning transmission electron microscope. In particular, it is shown that the nucleation of vanadium carbide precipitates often occurs at pre-existing titanium carbide precipitates which formed from titanium impurities in the bulk steel. This work will also highlight the links between the nanocharacterisation and changes in the bulk properties on annealing.

1. Introduction

The growing demand for increased fuel-efficiency in automotive applications is driving research on the development of higher strength ductile steels for body applications in order to reduce weight without compromising safety. One alloy system of interest for this application is a high-manganese (HiMn) steel microalloyed with either Nb or V to provide high densities of nanoscale carbide precipitates. Manganese stabilises the austenite phase and thereby increases ductility. The main characteristic of HiMn steels is their extraordinary combination of high tensile strength and ductility due to the work hardening effect [1-3], introducing additional dispersion hardening through the precipitation of nanosized carbides provides an effective way of further increasing strength. To effectively investigate the size, morphology and chemistry of such nanoscale precipitates, we are using scanning transmission electron microscopy, especially in combination with Electron Energy Loss Spectroscopy (EELS) and using the new DualEELS technique [4] to allow absolute quantification of the chemistry of nanosized precipitates. Clear differences are noted between precipitation behaviour in V and Nb microalloyed steels. In Nb steels, the precipitates are predominantly NbC_x and are noticeably faceted, and rather fine (typically 5-10 nm). In V steels, the precipitates are less strongly

faceted, slightly larger (often > 10 nm) and usually contain significant Ti impurities, possibly suggesting that they nucleate on pre-existing TiC precipitates.

2. Experimental

2.1. Materials and preparation

The base chemical composition of the alloy investigated is 20 wt. % Mn, 0.6 wt. % C, 1.5 wt. % Al, and balance Fe. We study two compositions microalloyed with either 0.1 wt. % Nb or 0.3 wt. % V. Transmission Electron Microscope (TEM) and Scanning Transmission Electron Microscope (STEM) specimen were prepared by Focused Ion Beam technique (FIB) using a FEI Nova 2000 DualBeam FIB (FEI, Eindhoven, NL).

2.2. Microscopy investigation

Precipitates were studied by STEM using a JEOL ARM200F equipped with a cold Field Emission Gun (FEG) source and operated at 200kV. EELS-spectrum imaging was performed using Gatan GIF Quantum 965 spectrometer using the DualEELS acquisition mode. Spectra were recorded using a 29mrad convergence semiangle and collection semiangles of either 36mrad or 72mrad. Atomic resolution HAADF imaging was also used to investigate the atomic structure and the faceting of the precipitates.

2.3. Post-processing procedure

The DualEELS technique makes it easy to use Fourier Deconvolution on an entire spectrum image, which makes it possible to remove the effects of plural scattering from core-loss edges, thereby enhancing the signal to background ratio and the reliability of quantification. We used a multistep procedure to process the data and to analyse the precipitates apart from the matrix. This starts by splicing the low loss and core loss spectra, followed by the reduction of noise using the weighted Principal Component Analysis (PCA) technique. It is then possible to deconvolute to remove plural scattering from each spectrum in the spectrum image. Finally, following [5], we calculated a matrix only spectrum image and subtracted this from the deconvoluted spectrum image to leave just a spectrum image of the precipitate. This final precipitate spectrum image could then be analysed using existing quantification routines to reveal precipitate chemistry and thickness without interference from the matrix.

3. Results and discussion

Figure 1a-d shows an example of the elemental maps of a typical carbide precipitate in a vanadium steel. One notable feature is the significant concentration of Ti throughout the particle, which is not an intentional part of the alloy. We had possibly expected to see the core shell structure, as this is commonly observed and published in the literature [6], which would arise if V nucleates on pre-existing TiN or TiC resulting from the interaction of Ti impurities from the foundry with C or N in the alloy. However in our case a range of thickness profiles for the different elements and the total inelastic scattering thickness are compared using the line shown on the inelastic thickness map in Figure 1 and these tell a different story. The Ti is evenly distributed through the particle, and the shape of its profile (blue line) has the same shape as the V profile (green). The thickness measured using the calibration of the mean free path with the Iakoubovskii formula [7] fits with expectations and shows a thickness close to the lateral dimensions. By comparing the thickness profiles for the different elements to this, it is clear that there are some systematic errors arising from incorrect cross-section estimation for the core-loss edges. The V profile follows the total thickness closely, when in reality it should be the V+ Ti thickness that matches the total thickness. This would indicate a slight underestimate of the V-$L_{2,3}$ and Ti-$L_{2,3}$ cross sections. However, considering that the quantification of both V and Ti is based on $L_{2,3}$ edges, we can probably trust ratios of Ti/V, and for different precipitates this has been observed to vary from 1:2.5 up to 1:4. These differences would probably lead to slight variations in lattice parameter from 4.16 Å up to 4.2 Å. The C profile follows the form of the thickness profile but is much higher, suggesting a significant underestimate of the C-K cross section

(especially as a metal carbide, $MC_{1-\delta}$, of this sort is likely to be substoichiometric with a noticeable C deficiency). It may be noted that there were some problems with background subtraction around the carbon edge which lead to negative counts outside the precipitate.

Figure 2 shows the results of a similar procedure when applied to a carbide precipitate in a Nb steel. As before, the total inelastic scattering thickness is consistent with the lateral dimensions of the particle and is probably reliable. In the precipitate, Nb and Ti is found and the form of their thickness traces matches well to the total thickness profile. As before, Ti substation occurs throughout the particle. Nevertheless, the absolute value of the thickness calculated for the Nb is very low, suggesting that there are systematic errors in the procedure. One likely source of error is an overestimate of the cross section for the Nb $M_{4,5}$ edge in Digital Micrograph. We also noted, however, that background subtraction for this edge is difficult due to the shape of the background before the edge not being well-behaved, possibly due to interference from the extended fine structure of lower energy edges. This can result in negative counts in some places, and these are particularly noticeable in the upper left of these maps. As before, the carbon thickness is significantly overestimated, suggesting again that the cross section for the C-K edge is significantly underestimated – this result has been consistently found in every precipitate we have mapped. Also, as before, carbon maps have significantly negative counts outside the precipitate due to background subtraction issues.

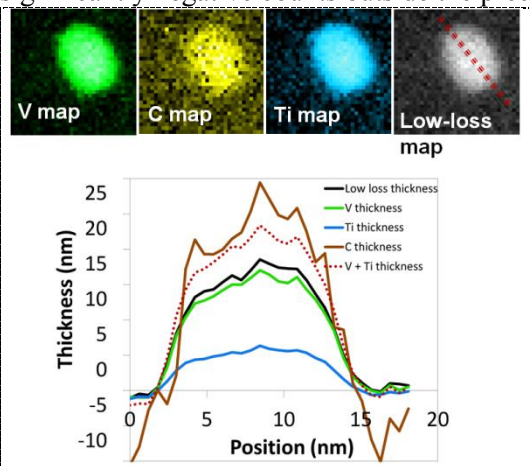

Figure 1. Maps with calculated thickness: a) V-$L_{2,3}$, b) C-K, c)Ti-$L_{2,3}$, d) calibrated inelastic scattering thickness, e) Profile of each thickness along the line drawn on d).

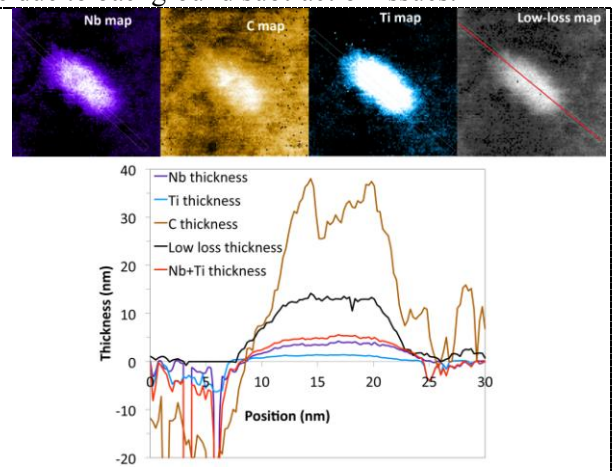

Figure 2. Maps with calculated thickness: a) Nb-$M_{4,5}$, b) C-K, c)Ti-$L_{2,3}$, d) calibrated inelastic scattering thickness, e) Profile of each thickness along the line drawn on d).

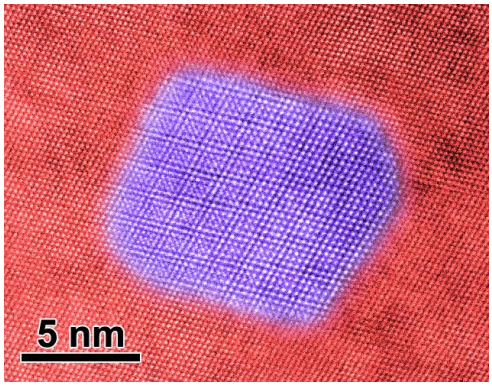

Figure 3. HRSTEM of Nb-particle, [011] direction.

An HRSTEM image of a NbC precipitate is presented in figure 3. HRSTEM can be used for evaluation of lattice parameter in the precipitate since there is a very clear lattice mismatch between precipitate and the matrix. Using the matrix lattice parameter of 3,668Å we can calculate the precipitate to have a lattice parameter of 4,41Å, which fits well with expectations for NbC [8]. The Nb precipitates have a tendency for strong faceting and the interface between matrix and precipitate is sharp on the following planes – (111), (200) and (220). The largest facets are on {111} planes, which are the close-packed planes in the face-centred cubic austenite, suggesting that strain can be minimised by forming semi-coherent interfaces on close-packed planes.

In the case of Vanadium steels, the imaging of precipitates is more difficult due to the lower Z of Vanadium, resulting in $(V,Ti)C_x$ precipitates appearing as darker than the austenite matrix. This makes HRSTEM extremely difficult in all but the thinnest areas, and consequently no detailed results can yet be presented on the interfaces of precipitates to the matrix in vanadium steels.

4. Conclusion

DualEELS spectroscopy allows absolute quantification of nanoscale precipitates in steels in terms of equivalent thicknesses of different elements, as well as total thickness from the total inelastic scattering. This also reveals that the cross sections used for quantifying elements in EELS are in need of correction. Future work will concentrate on accurate determination of partial cross sections for the elements found in our steels under the conditions used in this work.

The work reveals that nanoscale precipitates in V and Nb steels contain some fraction of Ti impurities in both cases, and it is likely that the Ti plays some role in the nucleation of the precipitation. In contrast to some studies, we found little evidence for core-shell structures involving Ti cores in precipitates. Atomic resolution STEM imaging also allowed us to investigate the faceting of NbC precipitates in some detail, showing preferential faceting to {111} planes, and also allowed us to measure the lattice parameter of these precipitates as 4,41 Å.

Acknowledgements

We are grateful to the European Commission for the funding of this work as part of a Research Fund for Coal and Steel Project (Precipitation in High Manganese Steels, RFSR-CT-2010-00018). This work was only possible because of the generous provision of the MagTEM facility by SUPA and the University of Glasgow.

References

[1] Bouaziz O *et al* 2011 High manganese austenitic twinning induced plasticity steels: A review of the microstructure properties relationships. Curr Opin Solid St M **15(4)** 141-168.
[2] Hamada, AS and Karjalainen LP 2011 Hot ductility behaviour of high-Mn TWIP steels. Mater Sci Eng A, **528(3**) 1819-1827.
[3] Sil'man GI 2006 Alloys of the Fe–C–Mn system part 4 special features of structure formation in manganese and high-manganese steels Met Sci heat treat+ **48(1-2)**.
[4] Scott J et al 2008 Near-simultaneous dual energy range EELS spectrum imaging. Ultramicroscopy **108 (12)** 1586-1594
[5] Craven AJ *et al* 2008 Spectrum imaging and three-dimensional atom probe studies of fine particles in a vanadium micro-alloyed steel Mat Sci Tech Ser **24(6)** 641-650.
[6] Show BK *et al* 2010 Effect of vanadium and titanium modification on the microstructure and mechanical properties of a microalloyed HSLA steel Mat Sci Eng A **527(6)** 1595-1604
[7] Iakoubovskii K *et al*.2008 Thickness measurements with electron energy loss spectroscopy Micros Res Techniq **71**(8) 626-31
[8] Tirumalasetty G K *et al* 2011 Characterisation of NbC and (Nb,Ti)N nanoprecipitates in TRIP assisted multiphase steels Acta Mater **59** 19 7406-7415